Title

Substrate specificity and ion coupling in the Na+/betaine symporter BetP

Journal

The EMBO Journal, 30(7)

ISSN

0261-4189

Authors

Perez, Camilo
Koshy, Caroline
Ressl, Susanne
et al.

Publication Date

2011-04-06

DOI

10.1038/emboj.2011.46

The EMBO Journal (2011) 30, 1221–1229 | © 2011 European Molecular Biology Organization | All Rights Reserved 0261-4189/11
www.embojournal.org

THE EMBO JOURNAL

Substrate specificity and ion coupling in the Na^+/betaine symporter BetP

Camilo Perez[1], Caroline Koshy[1], Susanne Ressl[1,2], Sascha Nicklisch[3,4], Reinhard Krämer[3] and Christine Ziegler[1,*]

[1]Department of Structural Biology, Max-Planck Institute of Biophysics, Frankfurt am Main, Germany, [2]Departments of Molecular and Cellular Physiology, Neurology and Neurological Sciences, Structural Biology, and Photon Science, The Howard Hughes Medical Institute, Stanford University, Stanford, CA, USA, [3]Institute of Biochemistry, University of Cologne, Köln, Germany and [4]Marine Science Institute, University of California, Santa Barbara, CA, USA

BetP is an Na^+-coupled betaine-specific transporter of the betaine–choline–carnitine (BCC) transporter family involved in the response to hyperosmotic stress. The crystal structure of BetP revealed an overall fold of two inverted structurally related repeats (LeuT-fold) that BetP shares with other sequence-unrelated Na^+-coupled symporters. Numerous structures of LeuT-fold transporters in distinct conformational states have contributed substantially to our understanding of the alternating access mechanism of transport. Nevertheless, coupling of substrate and co-transported ion fluxes has not been structurally corroborated to the same extent. We converted BetP by a single-point mutation—glycine to aspartate—into an H^+-coupled choline-specific transporter and solved the crystal structure of this mutant in complex with choline. The structure of BetP-G153D demonstrates a new inward-facing open conformation for BetP. Choline binding to a location close to the second, low-affinity sodium-binding site (Na2) of LeuT-fold transporters is facilitated by the introduced aspartate. Our data confirm the importance of a cation-binding site in BetP, playing a key role in a proposed molecular mechanism of Na^+ and H^+ coupling in BCC transporters.

The EMBO Journal (2011) **30,** 1221–1229. doi:10.1038/emboj.2011.46; Published online 1 March 2011
Subject Categories: membranes & transport; structural biology
Keywords: alternating access; H^+ and Na^+ coupling; inverted repeats; membrane transport; substrate specificity

Introduction

The betaine–choline–carnitine (BCC) transporter family comprises secondary carriers that facilitate the transport of a wide range of substrates that bear trimethylammonium groups ([-$N^+(CH_3)_3$]), such as betaine, choline, L-carnitine and γ-butyrobetaine (Ziegler *et al*, 2010). Although these substrates resemble each other structurally, they are transported by distinct coupling mechanisms. The zwitterionic betaine is co-transported with sodium (Farwick *et al*, 1995), the positively charged choline is co-transported with protons (Lamark *et al*, 1991) and L-carnitine is exchanged against γ-butyrobetaine by a sodium-independent antiport mechanism (Jung *et al*, 2002). Na^+- and H^+-coupled BCC symporters like BetP from *Corynebacterium glutamicum* and BetT from *Pseudomonas syringae* (Chen and Beattie, 2008) or *Escherichia coli* (Tøndervik and Strøm, 2007) are involved in the response to osmotic stress, regulating transport of osmolytes according to the external osmolality. BCC antiporters like the L-carnitine/γ-butyrobetaine antiporter CaiT from *E. coli* do not have a role in stress response (Jung *et al*, 2002). BetP is the best-characterized member of the BCCT family and the recently solved crystal structure (PDB entry 2WIT) (Ressl *et al*, 2009) has contributed to the understanding of osmolyte transport and stress-induced transporter activation (Krämer and Ziegler, 2009; Ziegler *et al*, 2010). BetP shares the so-called LeuT-fold of a 10 transmembrane (TM)-helix core formed by two inverted structurally related five TM-helix repeats with other sequence-unrelated transporters (Ziegler *et al*, 2010). Almost each individual structure of LeuT-fold transporters revealed a different conformational state of the alternating access cycle (Abramson and Wright, 2009). Two different models, the gating model and the rocker-switch model, describe conformational changes during transport based on the wealth of structural data (Forrest *et al*, 2010). Most recently, the conformations of both open states (outward facing and inward facing) were available for one single transporter, the Na^+-coupled hydantoin symporter Mhp1, revealing features of both, rocker-switch and gating model (Shimamura *et al*, 2010). However, the molecular mechanisms of alternating access in LeuT-fold transporters is still very much under debate especially the role of the first helix of the first repeat in the gating of substrate and co-substrate/counter-substrate-binding site (Boudker *et al*, 2007). Another intriguing question is the impact of the coupling ion on the substrate coordination, and thereby on the substrate specificity. BetP is highly specific for its only known substrate to date, betaine, which is transported with an apparent K_m of 3.5 μM (Rübenhagen *et al*, 2000). The crystal structure of BetP revealed aromatic residues from TM4 and TM8, which are conserved in all BCC transporters, coordinating the trimethylammonium group of betaine by cation–π interactions (Ressl *et al*, 2009). Subsequent structures reported for the BetP-homolog L-carnitine/γ-butyrobetaine antiporter CaiT (Schulze *et al*, 2010; Tang *et al*, 2010) confirmed the same aromatic binding motif for the trimethylammonium groups of L-carnitine and γ-butyrobetaine. Similar architectures of the aromatic binding sites in BetP and CaiT suggested that the exclusive specificity towards betaine in BetP is not related to the conserved residues in TM4 and TM8 (Ziegler *et al*, 2010). Residues in TM3 mediate binding of substrate carboxyl groups; however, the coordination differs signifi-

*Corresponding author. Department of Structural Biology, Max-Planck Institute of Biophysics, Max-von-Laue-Strasse 3, Frankfurt 60438, Germany. Tel.: +49 696 303 3054; Fax: +49 696 303 2209; E-mail: christine.ziegler@biophys.mpg.de

Received: 30 October 2010; accepted: 31 January 2011; published online: 1 March 2011

cantly for betaine (Ressl *et al*, 2009), L-carnitine (Tang *et al*, 2010) and γ-butyrobetaine (Schulze *et al*, 2010) reflected by the fact that residues in TM3 are only conserved for BCC transporters sharing the same substrate specificity (Ziegler *et al*, 2010). TM3, which corresponds to the first helix of the first repeat in BetP, carries a conserved motif of three glycines in its midsection (Ziegler *et al*, 2010). Here, we have investigated the role of the glycine stretch in substrate specificity and ion coupling. The flexibility of the stretch was changed systematically by point mutations. A single mutation of Gly153 to aspartate resulted in intriguing changes in substrate and co-substrate specificity. The mutant BetP-G153D showed choline transport not only driven by electrochemical sodium potential but also by proton motive force (pmf). Based on a 3.35-Å crystal structure of BetP-G153D in complex with choline, we describe a possible mechanism for the sodium and proton coupling in the BCCT family.

Results

Alanine scanning of the glycine stretch in TM3

Multiple sequence alignment (Figure 1A) indicates that the glycine motif (Gly149-x-Gly151-x-Gly153) located in the unwound region halfway across the membrane in TM3 (Figure 1B) defines Na^+-coupled betaine symporters in the BCCT family. We investigated this motif by an alanine scanning with respect to betaine transport activation upon an osmotic shock (Figure 1C and D). Replacement of Gly151 by alanine resulted in the strongest decrease in uptake rates of [^{14}C]-betaine in *E. coli MKH13* cells (Figure 1C) and a lack of activation at higher osmolalities. BetP-G149A although being significantly less active compared with the wild type (WT) still shows osmo-dependent activation. BetP-G153A retains WT activity at low osmolality; however, the activation profile is altered. Alanine exchange of the glycine motif significantly altered betaine transport, although it did not abolish it completely. The most drastic changes occur when the middle of the stretch is affected (Gly151; Figure 1B and C). Flexion of TM3 around its midsection might be part of a mechanism that renders the substrate-binding site accessible during conformational changes in the catalytic cycle. A similar conformational flexibility in the midsection of the first helix of the first repeat has been described previously for LeuT (Yamashita *et al*, 2005; Shi *et al*, 2008). Thus, we conclude that one important role of the glycine motif is to provide a functional conformational flexibility to TM3, which is the first helix of the first repeat in BetP in agreement with a mechanism described by the gating model (Zhao *et al*, 2010).

Sodium-coupled betaine and choline transport in BetP-G153D

In the choline-specific BCC transporter BetT, an aspartate residue lies in a position that corresponds to Gly153 in BetP (Figure 1A), while Gly149 and Gly151 are conserved. Choline and betaine are structurally very similar, both harbouring a positively charged trimethylammonium group (Figure 2A). However, betaine is zwitterionic comprising a negatively charged carboxyl group, while choline is positively charged due to its neutral hydroxyl group. We hypothesize that the presence of a negatively charged residue in TM3 is critical for choline to bind. Therefore, we introduce the point mutation G153D into BetP. In the presence of an electrochemical Na^+ potential, BetP-G153D transports betaine (Figure 2B), albeit with reduced affinity and V_{max} compared with the WT

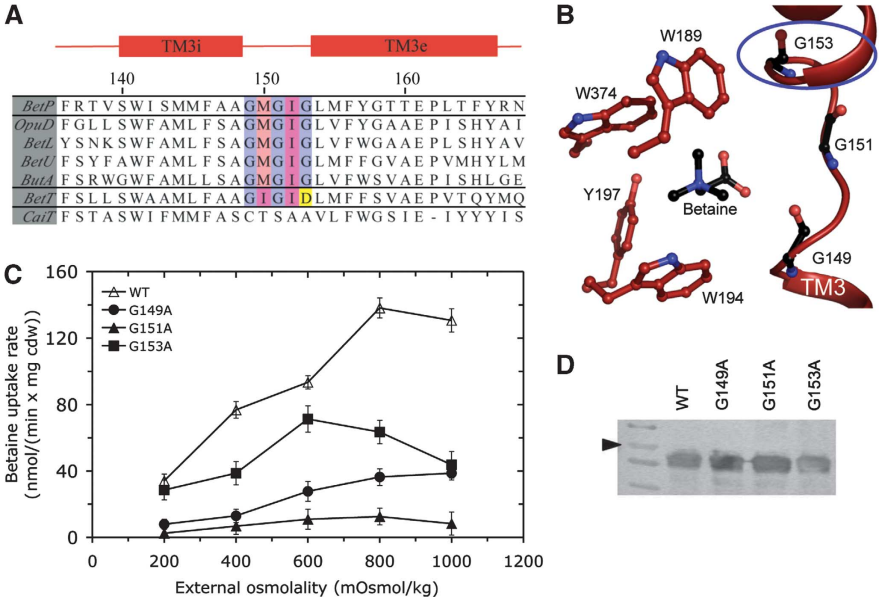

Figure 1 (**A**) Amino-acid sequence alignment of TM3 of *C. glutamicum* BetP to four Na^+/betaine transporters of the BCCT family; OpuD from *B. subtilis*, BetL from *Listeria monocytogenes*, BetU from *Proteus mirabilis*, ButA from *Tetragenococcus halophila*, the H^+/choline transporter BetT and the carnitine/γ-butyrobetaine antiporter CaiT both from *E. coli*. Residues in the unwound stretch of TM3 are shown in colours. α-Helical segments of TM3 are depicted as red bars on top of the sequence alignment. (**B**) The glycine motif in TM3 is shown together with the aromatic tryptophan box formed by Trp189, Trp194, Tyr197 and Trp374 from TM4 and TM8. (**C**). Uptake rates in nmol per min and mg cell dry weight (cdw) were measured dependent on the external osmolality in *E. coli MKH13* cells expressing BetP mutants with alanine substitutions in the flexible Gly-x-Gly-x-Gly motif. Each point shows the average of at least three independent experiments. The error bars represent s.d. (**D**) Immunoblotting against the N-terminal StrepII-tag of the different BetP variants in membranes of *E. coli MKH13* confirms approximately the same level of synthesis. The arrow indicates molecular weight marker of 72 kDa.

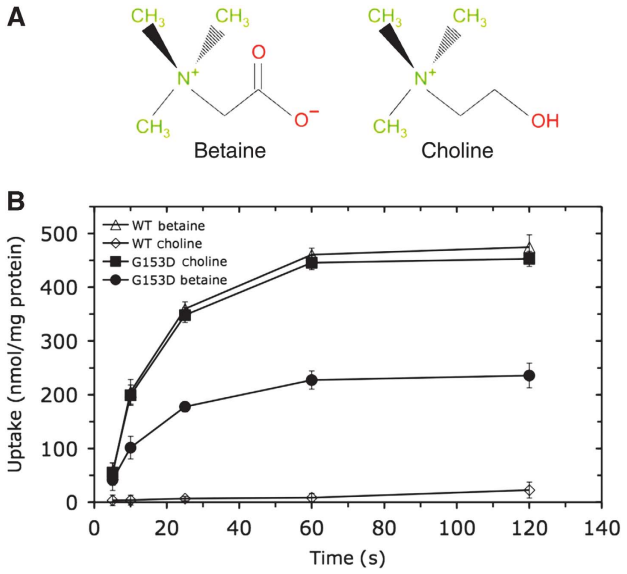

Figure 2 (**A**) Chemical structures of the zwitterionic betaine and the positively charged choline. (**B**) Na^+-coupled uptake of [^{14}C]-betaine and [^{14}C]-choline was measured for BetP WT and BetP-G153D, reconstituted in *E. coli* lipid proteoliposomes. Uptake was started by adding saturating concentrations of [^{14}C]-betaine (15 μM for BetP WT and 400 μM for BetP-G153D) or [^{14}C]-choline (400 μM for BetP WT and 400 μM for BetP-G153D) upon an osmotic shock of 600 mOsmol/kg adjusted with proline. Each value shows the average of three independent measurements. The error bars represent s.d.

Table I Kinetic constants of BetP wild type (WT), BetP-G153D and BetP-G153D/W189Y

	K_m (μM)	V_{max} (nmol/min × mg protein)	K_{cat} (/min)
Na^+ potential			
WT			
Betaine	3.5 ± 0.6	2264 ± 93	147 ± 6
Choline	BD[a]	BD	BD
G153D			
Betaine	63 ± 13	816 ± 78	53 ± 5
Choline	138 ± 11	2299 ± 85	149 ± 6
G153D/W189Y			
Betaine	57 ± 15	803 ± 64	52 ± 4
Choline	125 ± 9	2192 ± 76	142 ± 5
H^+ potential			
G153D			
Choline	35 ± 9	1047 ± 73	68 ± 5
G153D/W189Y			
Choline	33 ± 10	1123 ± 87	73 ± 6

[a]Below detection (BD). Each value represents the average ± s.d. of three independent measurements.

protein when measured in proteoliposomes (Table I). By assuming that betaine transport is similarly catalysed in BetP and in BetP-G153D, the decreased affinity of the mutant form towards betaine might be caused by the decreased flexibility of the unfolded stretch in TM3. Further, BetP-G153D also transports choline (Figure 2B), while choline transport was not detected in the WT. The transport rate for choline in BetP-G153D was comparable to that of betaine in the WT, although the affinity of BetP-G153D for choline in the presence of sodium was significantly lower than for betaine (Table I). One of the tryptophans contributing to the substrate-binding site was exchanged against a tyrosine that is the corresponding residue found in BetT at the same location (W189Y in TM4 of Supplementary Figure S1A). However, this additional mutation in the aromatic binding box did not cause any further significant change in the kinetics of Na^+-coupled betaine or choline transport (Table I). We suggest that to the inserted aspartate has the key role in the coordination of choline during Na^+-coupled transport. A similar coordination of choline by hydrogen bonds with an aspartate residue was reported earlier in the choline-binding protein ChoX of the ABC transporter ChoXWU from *E. coli* (Oswald *et al*, 2008) (Supplementary Figure S1B).

Proton-coupled transport of BetP-G153D

BetT, in contrast to BetP, is a proton-coupled symporter (Lamark *et al*, 1991). Proton coupling and translocation is assumed to involve charged residues, which might be protonated during transport. With regard to the *E. coli* H^+-coupled lactose symporter LacY, approximately five charged residues have been proposed to coordinate proton translocation (Smirnova *et al*, 2009). BetT does not harbour any additional charged residues along the putative substrate translocation pathway when compared with BetP. Asp97 in TM3 of BetT is the only charged residue in this context and therefore the most likely to be critically involved in proton translocation by BetT.

Transport of betaine and choline in BetP WT and BetP-G153D energized by pmf was measured in *E. coli* lipid proteoliposomes. In BetP-G153D choline transport could indeed be coupled to the electrochemical proton gradient (Figure 3A) and abolished in the absence of an inwardly directed proton gradient (Figure 3B). Transport rates decreased to ∼25% in the presence of the protonophore CCCP (Figure 3B). The apparent K_m for choline in BetP-G153D decreased to 35 μM in the presence of protons (Table I). Neither BetP-G153D nor the WT catalysed the co-transport of betaine with protons, and the WT failed to co-transport choline with protons, too. Due to the differences in ΔG values, when transport is driven by pmf and smf of different extent, proton-coupled choline transport activity cannot quantitatively be compared with Na^+-coupled choline or betaine transport activity; however, they seem to be in at least a similar range. We conclude that a single-point mutation is sufficient to convert BetP from an Na^+-coupled betaine-specific transporter to an H^+-coupled choline-specific transporter. In the presence of sodium, this mutant transports betaine and choline. Therefore, a single residue in TM3 determines both substrate and co-substrate specificity in a BCC transporter, pointing towards a common molecular mechanism of Na^+ and H^+ coupling in this transporter family.

Structure of BetP-G153D

The mutation G153D was introduced in the N-terminally truncated BetPΔN29 and 3D crystals were grown in excess of choline. The structure of BetPΔN29G153D (PDB entry 3PO3) was solved to 3.35 Å (Table II), without imposition of a three-fold non-crystallographic symmetry to account for the conformational asymmetry of individual protomers within the trimer (Tsai *et al*, 2011). A choline molecule was observed in one of the three protomers within the trimer (light blue protomer in Figure 4A) located in a central binding site that is fully accessible from the cytoplasm (Figure 4B). This open inward-facing state constitutes a new conformation

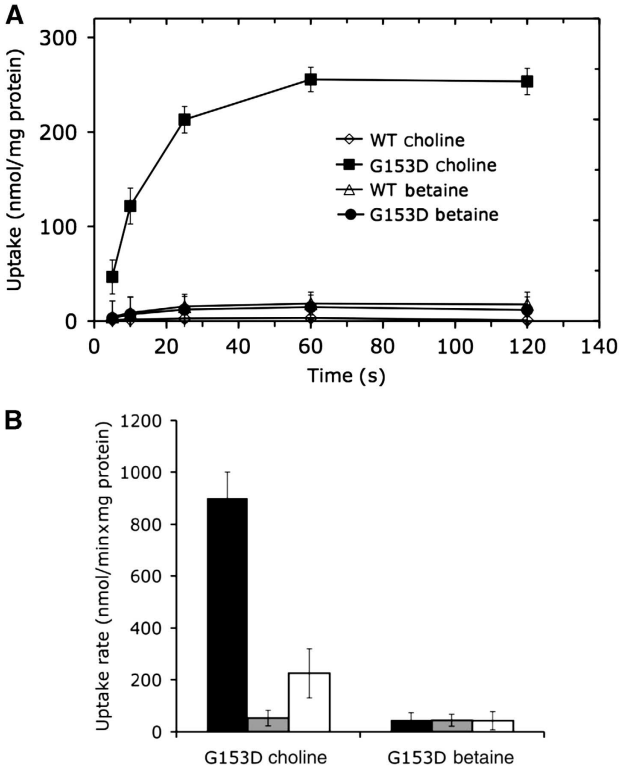

Figure 3 (**A**) Proton-coupled transport of betaine and choline by BetP WT and BetP-G153D, reconstituted in *E. coli* lipid proteoliposomes. Uptake was energized by a proton gradient of pH 5.5_{out}/7.5_{in}. Each value shows the average of three independent measurements. The error bars represent s.d. (**B**) BetP-G153D-catalysed uptake rates of [^{14}C]-betaine and [^{14}C]-choline in the presence of a pH gradient of pH $5.5_{out}/7.5_{in}$ (black bars), in the absence of pH gradient at pH $7.5_{out}/7.5_{in}$ (grey bars), and in the presence of a pH gradient and 10 μM CCCP (carbonyl cyanide *m*-chlorophenylhydrazone) (white bars). In both figures, each value represents an average of three independent measurements. The error bars show the s.d.

Table II Data collection and refinement statistics of BetP-G153D (PDB entry 3PO3)

Data collection	
Space group	$P2_12_12_1$
Cell dimensions	
a, *b*, *c* (Å)	117.56, 129.31, 183.14
α, β, γ (deg)	90, 90, 90
Resolution (Å)[a]	46.2–3.35 (3.5–3.35)
R_{merge} [a]	0.122 (0.804)
$I/\sigma I$[a]	14.5 (3.1)
Completeness (%)[a]	91.2
Refinement	
Resolution (Å)	46.2–3.35
No. of reflections	37219
R_{work}/R_{free} (%)[b]	24.46/30.04
R.m.s.d.[c] bonds (Å)	0.007
R.m.s.d. angles (deg)	1.110

[a]Values in parentheses refer to data in the highest resolution shell.
[b]$R_{work} = \Delta\Sigma||Fobs–Fcalc||/\Sigma|Fobs|$. The R_{free}, is the same as the R_{work} but for 10% of the data that were excluded from the refinement.
[c]R.m.s.d., root mean square deviation.

of BetP in comparison to the betaine-bound structure of BetP (PDB entry 2WIT) (Figure 4B) reported previously as occluded state (Ressl *et al*, 2009). In the light of the open inward-facing state observed for BetP-G153D, hereafter, we will refer to the betaine-bound structure (PDB entry 2WIT) as occluded inward-facing conformation. Superimposition of both structures (Figure 4C) supports a rigid-body movement of the bundle domain (first two helices of each repeat) relative to the scaffold of adjacent helices (helices 3 and 4 of each repeat) that is comparable to the conformational changes described very recently for vSGLT (Supplementary Table SI) (Watanabe *et al*, 2010). The intracellular halves of TM3 and TM8 are displaced by 6° and 5°, respectively (Figure 4C). Side chain displacements of residues Ala144, Met144, Ile302, Gln303, Phe380, Phe384, Ile388 and Ser471 facilitate the accessibility of the binding site from the cytoplasm (Figure 4C, inset). The substrate choline binds by a hydrogen bond formed by its hydroxyl group with the carboxyl group of Asp153 (Figure 5A and B) located at the end of the unwound region in TM3. The trimethylammonium group is coordinated by the carbonyl groups of Ala148 and Met150 in TM3, by Van der Waals interactions with Trp377 and Phe380 in TM8, and by the hydroxyl group of Ser468 in TM10. Trp377 is a crucial residue in substrate transport in BetP and replacement against leucine abolished betaine transport (Ressl *et al*, 2009). Asp153 forms an additional hydrogen bond to Ser253 in TM5. In the inward-facing open conformation, the positively charged trimethylammonium group of choline is located close to the position of one of the potential sodium-binding sites (Supplementary Figure S2A). This site corresponds to the Na2 site in the outward-facing state of LeuT (Yamashita *et al*, 2005) (Supplementary Figure S2B). In comparison to the betaine location in the occluded inward-facing betaine-bound state of BetP, choline is not located in the aromatic box formed by residues from TM4 and TM8. This shift in substrate-binding site is reflected by subtle changes in the positions of Trp189, Trp377 and Phe380 as observed in the superimposition of inward-facing occluded and inward-facing open states (Figure 6).

Discussion

Structural data on several transporters revealed that a few key amino-acid residues determine substrate specificity in secondary transporters (Forrest *et al*, 2010). Corresponding point mutations led to a change in substrate specificity for example in the glycerol-3-phosphate: phosphate antiporter GlpT (Law *et al*, 2009) or in the creatine transporter (Dodd and Christie, 2007). BetP alters substrate specificity even by only a single-point mutation. The crystal structure of BetP-G153D provides evidence for how choline transport is enabled by the presence of the strategically positioned Asp153 in TM3. However, the most intriguing consequence of this mutation is the switching to another coupling ion, which allows speculating about a common mechanism of Na^+ and H^+ coupling in BCC transporters. The presence of a cation-binding site that might serve for different mechanistic purposes appears to be the key parameter for a possibility of simultaneous sodium and proton coupling in transporters of the BCCT family. The BetP-G153D structure suggests this site at a position assigned as Na2 sodium-binding site (Supplementary Figure S2A). Na2 is conserved in five TM-helix repeat transporters including vSGLT (Faham *et al*, 2008), Mhp1 (Weyand *et al*, 2008) and BetP (Ressl *et al*, 2009) and was first reported in the 1.65-Å structure of the leucine transporter LeuT (PDB entry 2AS5)

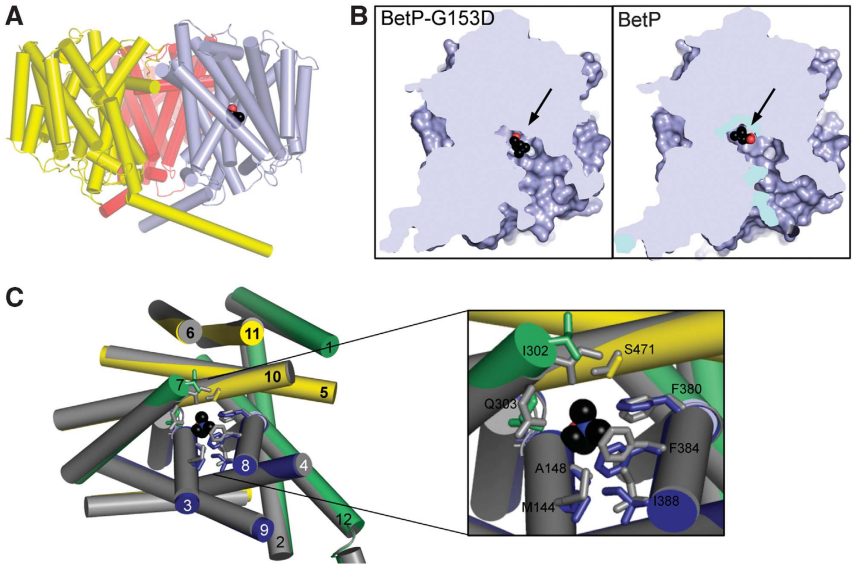

Figure 4 BetP-G153D structure. (**A**) Side view of BetP-G153D trimer composed of protomer A (yellow), protomer B (red) and protomer C (light blue). Choline (black) is bound to protomer C. (**B**) Comparison of the inward-facing open state of BetP-G153D and the occluded inward-facing state of BetP (PDB entry 2WIT) viewed by a section through the protein volume. Choline and betaine are shown in black spheres and pointed by an arrow. (**C**) Overlay of the occluded inward-facing state (grey) and the inward-facing open state (bundle domain in blue; hash domain in yellow; peripheral helices in green). (Inset) Conformational changes of individual side chains alter the accessibility towards the binding site from the cytoplasm.

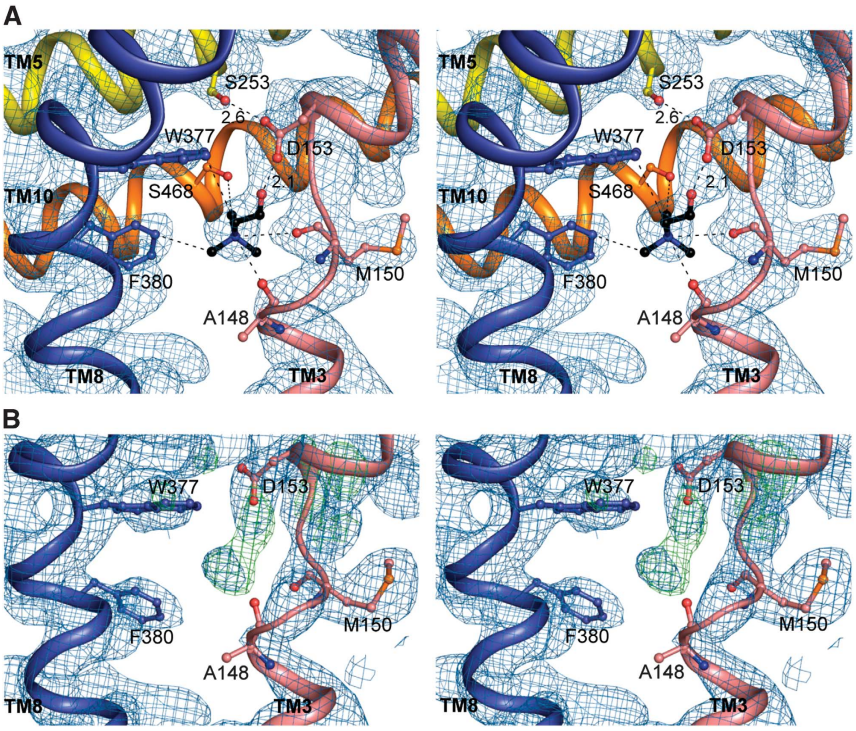

Figure 5 Stereoview of the BetP-G153D choline-binding site. (**A**) The $2F_o$–F_c map (blue) of the choline-binding site contoured at 1.4σ is shown with choline (black) in stick representation. TM helices are shown in spiral presentation with TM3 (salmon), TM5 (yellow) and TM8 (dark blue). TM10 (orange) is displayed without density for visual clarity. Ala148, Met150, Asp153, Trp377, Phe380 and Ser468 coordinate the choline molecule. Hydrogen bonds and Van der Waals interactions are depicted as dashed lines. (**B**) $2F_o$–F_c (blue) and F_o–F_c (green) map contoured at 1.4σ and 3.0σ, respectively, of the choline-binding site in an early refinement round in which choline was not positioned yet.

(Yamashita *et al*, 2005) (Supplementary Figure S2B). The Na2 sodium is situated between the 4TM-helix bundle formed by the two first helices of each repeat (helices 1 and 6 in Figure 7A) and the hash domain comprising the third and fourth helix of each repeat (helices 3 and 8 in Figure 7A). Molecular dynamics free energy calculations (Caplan *et al*, 2008; Shi *et al*, 2008) on LeuT designated the Na2 site as a relatively weak binding site. It was shown recently that the electrostatic component provided by a cation in the Na2 site is crucial in opening the external gates in LeuT-fold transporters (Shaffer *et al*, 2009). These electrostatic interactions can also be provided by fixed side chain charges. In ApcT, an

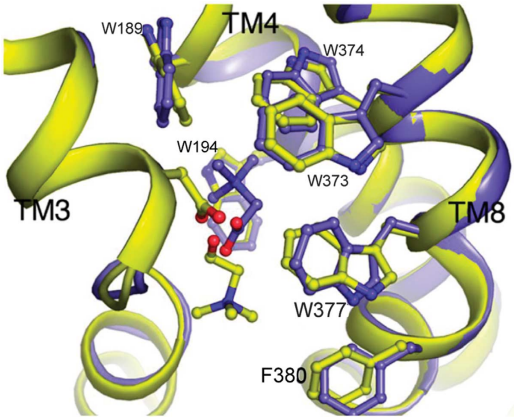

Figure 6 Superimposition of aromatic residues in TM3, TM4 and TM8 of BetP-G153D (yellow) and BetP (PDB entry 2WIT) (blue) contributing to the respective binding pockets of choline in BetP-G153D and betaine in BetP. Subtle conformational changes of Trp189, Trp377 and Phe380 are observed. The trimethylammonium group of betaine is located in an aromatic pocket (Trp189, Trp194, Trp374 and Trp373), and the trimethylammonium group of choline is located at the Na2 site.

H^+-coupled amino-acid transporter also of the LeuT-fold, a positively charged lysine (Lys158) is located at the Na2 site, and its protonation might mimic a monovalent cation (Shaffer *et al*, 2009).

Analogous to LeuT and ApcT, we suggest that in BetP, the binding of sodium to the Na2 site in the outward-facing open conformation (C_e-state in Figure 7A) triggers flexion of the periplasmic half of TM3 around its glycine-rich extended stretch. Thereby, the aromatic box turns accessible for the substrate (C_e*-state) by opening an extracellular gate (Figure 7A, red bar), although this is rather speculative since an outward-facing structure of BetP is unknown. Subsequently, betaine or choline binds to the central binding site ($S_{oc}C_e$-state). In LeuT, another sodium ion occupies a high-affinity sodium-binding site (Na1) that stabilizes TM6 (Yamashita *et al*, 2005) and provides an electrostatic coordination for the carboxyl group of leucine. Since transport in BetP requires two sodium ions per betaine molecule, it was assumed that the carboxyl group of betaine is similarly coordinated ($S_{oc}C_e$-state for BetP in Figure 7A). The exact position of this putative Na1 site was not yet assigned for BetP. However for BetP-G153D, Asp153 purveys an electrostatic component to coordinate the hydroxyl group of choline similar to the coordination observed in the periplasmic choline-binding protein ChoX (Oswald *et al*, 2008) (Supplementary Figure S1B). In this scenario, choline flux is still coupled to the sodium flux and sodium stoichoimetry might even not change since the Na1 site is not affected by the mutation in TM3. The main difference is that choline might not be coordinated any longer by sodium.

In the same context, we suggest that binding of the bulky cationic ammonium group of choline to the Na2 site, which would function as a monovalent cation-binding site in that case, opens the extracellular gate in the absence of sodium (transition of C_e- to SC_e-state in Figure 7B). The observed lower affinity for choline in the presence of sodium would be caused by competition between the positive charges of choline and sodium for the Na2-binding site, suggesting that Na^+ has an inhibitory effect during H^+-coupled transport. At some stage during the alternating access cycle, the trimethylammonium group of choline might be positioned in the aromatic pocket similar to what we predict for choline binding ($S_{oc}C_i$-state in Figure 7B) based on a homology model of BetT (Supplementary Figure S3A).

The structural and functional data presented here indicate that the key parameter in H^+-coupled choline transport is the protonation of the aspartate residue. Most likely, the pKa of Asp153 has to shift significantly in different states of the transport cycle. Based on pKa predictions (Li *et al*, 2005) it can be assumed that on coordination to choline, the pKa of the aspartate shifts to 4.4, therefore Asp153 will be deprotonated at pH 5.5 (transition from SC_e- to $S_{oc}C_e$-state in Figure 7B). Subsequently, it might be possible that release of a proton triggers the conformational change from outward to inward-facing conformation and the predicted pKa of Asp153 would rise to 6.5 once choline is released, resulting in protonation of the carboxyl group. The interaction between Asp153 and Ser253, which represents a link between the bundle and the hash domain, might be also important during a conformational change back to an outward-facing state (Supplementary Figure S3B; transition of C_i- to C_e-state in Figure 7B). Obviously, protonation of Asp153 has a different role in the transport cycle of BetP compared with Lys158 in ApcT, where protonation of this residue renders the central binding site accessible for the substrate (Shaffer *et al*, 2009).

How protons in BetP-G153D are transported in a pathway that is initially designed for sodium remains unknown. In LacY, the binding of lactose requires prior protonation of specific residues (Smirnova *et al*, 2009), and substrate affinity is pH dependent; both events have been observed during H^+-coupled choline binding in BetP-G153D. Moreover, no additional charges line the lactose pathway, and water molecules are proposed to act as a co-factor in LacY during proton translocation by forming a transient hydronium ion (Smirnova *et al*, 2009). Hydronium is assumed to pass via similar pathways as the sugar in LacY. In BetP-G153D, a similar mechanism might be possible assuming that a hydronium ion occupies similar positions as choline at different time points in the catalytic cycle (Figure 7B).

Collectively, our data suggest a rather similar mechanism for Na^+ and H^+ coupling in BCC transporters. In the initial step, a cation (sodium or choline) is bound in the Na2 site thereby opening an extracellular gate to render the substrate-binding site accessible. Subsequently, a coupling ion might contribute to the generation of the substrate-binding site directly by interacting with the substrate (Na^+ binding to the Na1 site when betaine is the substrate) or, alternatively, a charged residue may mimic this event (choline coordination by aspartate). The primary requirement for H^+ coupling, however, compared with Na^+ coupling, is the presence of a side chain that undergoes pKa shifts after conformation-induced interactions (Ser253–Asp153) or on interaction with the substrate (Asp153–choline), respectively. By this means, BCC transporters seem to maintain certain promiscuity towards their coupling ion in the case of a cationic substrate.

Materials and methods

E. coli DH5αmcr were used for the heterologous expression of *strep-betp*. The QuikChange™ kit (Stratagene), in combina-

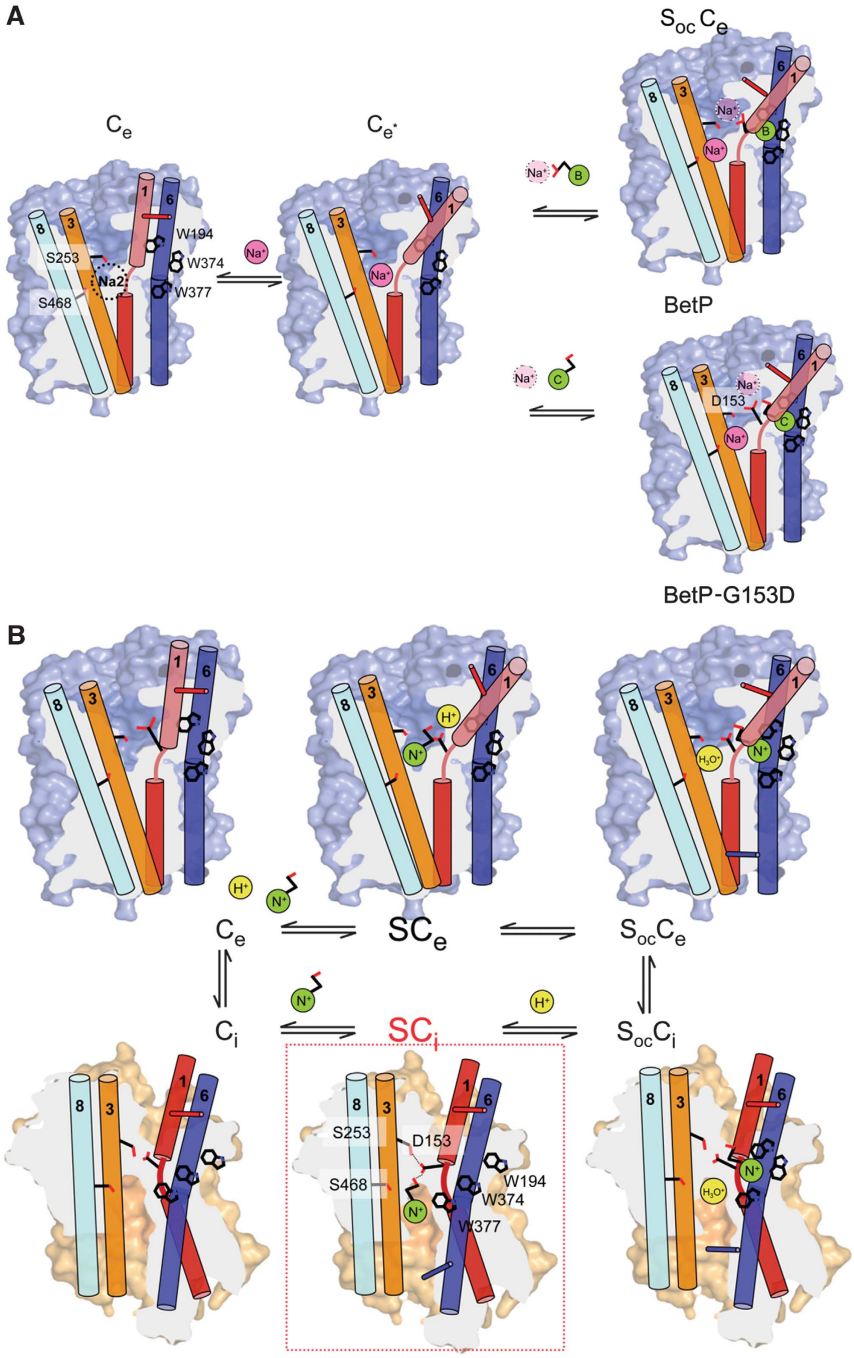

Figure 7 (**A**) Proposed Na^+-coupled betaine and choline binding in BetP and BetP-G153D. Shown are the first helices of each repeat (bundle): 1 (red) and 6 (dark blue); and the third helix of each repeat (hash domain): 3 (orange) and 8 (light blue) according to LeuT nomenclature for better comparison. The dashed circle in the outward-facing open state (C_e-state) assign the position of Na2 sodium-binding site. A putative extracellular gate is shown as red bar in the C_e-state, in a transient outward-facing state with the extracellular gate open (C_e*-state) and in the substrate occluded outward-facing state ($S_{oc}C_e$-state). Pink spheres represent sodium ions occupying the Na2 site, and green circles represent the trimethylammonium group of betaine and choline. The light pink spheres represent sodium that might occupy a putative Na1 site to coordinate the carboxyl group of the substrate ($S_{oc}C_e$-state in BetP). (**B**) Proposed H^+-coupled choline transport in BetP-G153D. Binding of cationic choline to the Na2 sodium-binding site might open the extracellular gate (SC_e-state). $S_{oc}C_i$- and SC_i-states assign for a substrate occluded inward-facing state and for a substrate bound inward open state, respectively. SC_i-state corresponds to the conformation of the crystal structure and is labelled by a red box. C_i-state stands for the inward-facing open state. A putative intracellular gate is shown as blue bar located at the cytoplasmic half of the first helix of the second repeat.

tion with *Pfu* Turbo DNA polymerase, was used for the replacement of nucleotides in the pASK-IBA5betP and pASK IBA7betPDeltaN29EEE44/45/46AAA plasmids (Schiller *et al*, 2004). Membranes were solubilized using β-dodecyl-maltoside, and BetP was purified by affinity chromatography via Strep-Tactin macroprep and size exclusion chromatography (Ziegler *et al*, 2004; Ressl *et al*, 2009). Uptake of labelled betaine and choline was measured in *E. coli MKH13* cells and proteoliposomes made of *E. coli* polar lipids (Ott *et al*, 2008) started by adding 15–400 μM of [^{14}C]-betaine or [^{14}C]-choline

upon an osmotic shock of 600 mOsmol/kg adjusted with proline. When transport was energized by an electrochemical proton gradient, the internal buffer composed 100 mM KPi at pH 7.5 and the external buffer 100 mM KPi at pH 5.5, 50 mM MES at pH 5.5 and 10 nM valinomycin. The kinetic constants were derived by Michaelis–Menten curve fitting of the uptake rates versus substrate concentration with GraphPad Prism version 5.0c for Mac OS X (Motulsky, 1999). BetPDeltaN29/G153D was crystallized in the presence of choline. A data set to 3.35 Å was collected at ESRF-ID29, and the crystal structure was determined by molecular replacement against the structure of Chain C of BetP (PDB entry 2WIT). The substrate was positioned when a clear positive peak in the F_o–F_c difference electron-density map was observed in the binding site after several refinement rounds. Extended version of the methods is given as supporting information.

Supplementary data

Supplementary data are available at *The EMBO Journal* Online (http://www.embojournal.org).

Acknowledgements

We thank Özkan Yildiz for support with the crystallography and model building and Lucy Forrest for helpful discussions and suggestions. Vera Ott made valuable suggestions on the BetP transport experiments. We thank the beam line scientists at the SLS PX-II at the ESRF-ID29, who helped during initial screening and data collection. This work was supported by the International Max-Planck Research School, Frankfurt, and by the DFG (German Research Foundation), Collaborative Research Center 807, Transport and Communication across Biological Membranes.

Author contributions: CP performed all mutations, the activity measurements in cells and proteoliposomes, and crystallization and collected and processed the data; CK carried out the homology modelling; SR directed CP in the early X-ray experiments and performed the initial crystallographic data analysis; SN made initial proteoliposome measurements; CP and CZ analysed the data; CZ directed the research; and CP, RK and CZ wrote the paper.

Author information: Coordinates and structure factors for BetP-G153D with bound substrate (PDB entry 3PO3) have been deposited into the Protein Data Bank.

Conflict of interest

The authors declare that they have no conflict of interest.

References

Abramson J, Wright EM (2009) Structure and function of Na(+)-symporters with inverted repeats. *Curr Opin Struct Biol* **19:** 425–432

Boudker O, Ryan RM, Yernool D, Shimamoto K, Gouaux E (2007) Coupling substrate and ion binding to extracellular gate of a sodium-dependent aspartate transporter. *Nature* **445:** 387–393

Caplan D, Subbotina J, Noskov S (2008) Molecular mechanism of ion-ion and ion-substrate coupling in the Na^+-dependent leucine transporter LeuT. *Biophys J* **95:** 4613–4621

Chen C, Beattie GA (2008) Pseudomonas syringae BetT is a low-affinity choline transporter that is responsible for superior osmoprotection by choline over glycine betaine. *J Bacteriol* **190:** 2717–2725

Dodd J, Christie D (2007) Selective amino acid substitutions convert the creatine transporter to a gamma-aminobutyric acid transporter. *J Biol Chem* **282:** 15528–15533

Faham S, Watanabe A, Besserer G, Cascio D, Specht A, Hirayama B, Wright E, Abramson J (2008) The crystal structure of a sodium galactose transporter reveals mechanistic insights into Na^+/sugar symport. *Science* **321:** 810–814

Farwick M, Siewe R, Kramer R (1995) Glycine betaine uptake after hyperosmotic shift in *Corynebacterium glutamicum*. *J Bacteriol* **177:** 4690–4695

Forrest LR, Krämer R, Ziegler C (2010) The structural basis of secondary active transport mechanisms. *Biochim Biophys Acta* **1807:** 167–188

Jung H, Buchholz M, Clausen J, Nietschke M, Revermann A, Schmid R, Jung K (2002) CaiT of *Escherichia coli*, a new transporter catalyzing L-carnitine/gamma-butyrobetaine exchange. *J Biol Chem* **277:** 39251–39258

Krämer R, Ziegler C (2009) Regulative interactions of the osmosensing C-terminal domain in the trimeric glycine betaine transporter BetP from *Corynebacterium glutamicum*. *Biol Chem* **390:** 685–691

Lamark T, Kaasen I, Eshoo M, Falkenberg P, McDougall J, Strøm A (1991) DNA sequence and analysis of the bet genes encoding the osmoregulatory choline glycine betaine pathway of *Escherichia coli*. *Mol Microbiol* **5:** 1049–1064

Law C, Enkavi G, Wang D, Tajkhorshid E (2009) Structural basis of substrate selectivity in the glycerol-3-phosphate: phosphate antiporter GlpT. *Biophys J* **97:** 1346–1353

Li H, Robertson A, Jensen H (2005) Very fast empirical prediction and interpretation of protein pKa values. *Proteins* **61:** 704–721

Motulsky H (1999) *Analyzing Data with GraphPad Prism*. GraphPad Software Inc.: San Diego, CA, http://www.graphpad.com

Oswald C, Smits S, Höing M, Sohn-Bösser L, Dupont L, Le Rudulier D, Schmitt L, Bremer E (2008) Crystal structures of the choline/acetylcholine substrate-binding protein ChoX from *Sinorhizobium meliloti* in the liganded and unliganded-closed states. *J Biol Chem* **283:** 32848–32859

Ott V, Koch J, Späte K, Morbach S, Krämer R (2008) Regulatory properties and interaction of the C- and N-terminal Domains of BetP, an osmoregulated betaine transporter from *Corynebacterium glutamicum*. *Biochemistry* **47:** 12208–12218

Ressl S, Terwisscha van Scheltinga A, Vonrhein C, Ott V, Ziegler C (2009) Molecular basis of transport and regulation in the Na^+/betaine symporter BetP. *Nature* **458:** 47–53

Rübenhagen R, Rönsch H, Jung H, Krämer R, Morbach S (2000) Osmosensor and osmoregulator properties of the betaine carrier BetP from *Corynebaterium glutamicum* in proteoliposomes. *J Biol Chem* **275:** 735–741

Schiller D, Rübenhagen R, Krämer R, Morbach S (2004) The C-terminal domain of the betaine carrier BetP of *Corynebacterium glutamicum* is directly involved in sensing K^+ as an osmotic stimulus. *Biochemistry* **43:** 5583–5591

Schulze S, Köster S, Geldmacher U, Terwisscha van Scheltinga A, Kühlbrandt W (2010) Structural basis of Na^+-independent and cooperative substrate/product antiport in CaiT. *Nature* **467:** 233–236

Shaffer P, Goehring A, Shankaranarayanan A, Gouaux E (2009) Structure and mechanism of a Na^+-independent amino acid transporter. *Science* **325:** 1010–1014

Shi L, Quick M, Zhao Y, Weinstein H, Javitch J (2008) The mechanism of a neurotransmitter:sodium symporter inward release of Na^+ and substrate is triggered by substrate in a second binding site. *Mol Cell* **30:** 667–677

Shimamura T, Weyand S, Beckstein O, Rutherford N, Hadden J, Sharples D, Sansom M, Iwata S, Henderson P, Cameron A (2010) Molecular basis of alternating access membrane transport by the sodium-hydantoin transporter Mhp1. *Science* **328:** 470–473

Smirnova I, Kasho V, Sugihara J, Choe J, Kaback H (2009) Residues in the H^+ translocation site define the pK_a for sugar binding to LacY. *Biochemistry* **48:** 8852–8860

Tøndervik A, Strøm A (2007) Membrane topology and mutational analysis of the osmotically activated BetT choline transporter of *Escherichia coli*. *Microbiology* **153:** 803–813

Tang L, Bai L, Wang W, Jiang T (2010) Crystal structure of the carnitine transporter and insights into the antiport mechanism. *Nat Struct Mol Biol* **17:** 492–496

Tsai CJ, Khafizov K, Hakulinen J, Forrest LR, Krämer R, Kühlbrandt W, Ziegler C (2011) Structural asymmetry in a trimeric Na^+/betaine symporter BetP from *Corynebacterium glutamicum*. *J Mol*

Biol (advance online publication, 31 January 2011; doi:10.1016/j.jmb.2011.01.028)

Watanabe A, Choe S, Chaptal V, Rosenberg JM, Wright EM, Grabe M, Abramson J (2010) The mechanism of sodium and substrate release from the binding pocket of vSGLT. *Nature* **468:** 988–991

Weyand S, Shimamura T, Yajima S, Suzuki S, Mirza O, Krusong K, Carpenter E, Rutherford N, Hadden J, O'Reilly J, Ma P, Saidijam M, Patching S, Hope R, Norbertczak H, Roach P, Iwata S, Henderson P, Cameron A (2008) Structure and molecular mechanism of a nucleobase-cation-symport-1 family transporter. *Science* **322:** 709–713

Yamashita A, Singh S, Kawate T, Jin Y, Gouaux E (2005) Crystal structure of a bacterial homologue of Na^+/Cl^- dependent neurotransmitter transporters. *Nature* **437:** 215–223

Zhao Y, Terry D, Shi L, Weinstein H, Blanchard S, Javitch J (2010) Single molecule dynamics of gating in a neurotransmitter transporter homologue. *Nature* **465:** 188–193

Ziegler C, Bremer E, Krämer R (2010) The BCCT family of carriers: from physiology to crystal structure. *Mol Microbiol* **78:** 13–34

Ziegler C, Morbach S, Schiller D, Krämer R, Tziatzios C, Schubert D, Kühlbrandt W (2004) Projection structure and oligomeric state of the osmoregulated sodium/glycine betaine symporter BetP of *Corynebacterium glutamicum*. *J Mol Biol* **337:** 1137–1147